T. KOZIEŁ*, J. LATUCH**, A. ZIELIŃSKA-LIPIEC*

STRUCTURE OF THE AMORPHOUS-CRYSTALLINE $Fe_{66}Cu_6B_{19}Si_5Nb_4$ ALLOY OBTAINED BY THE MELT-SPINNING PROCESS

STRUKTURA AMORFICZNO-KRYSTALICZNEGO STOPU $Fe_{66}Cu_6B_{19}Si_5Nb_4$ OTRZYMANEGO METODĄ MELT-SPINNING

This paper presents structure investigations of the rapidly cooled $Fe_{66}Cu_6B_{19}Si_5Nb_4$ alloy. A proper selection of chemical composition enabled in-situ formation of the amorphous-crystalline composite during the melt spinning process. Liquid phase separation into the Fe-rich and the Cu-rich phases was confirmed. The microstructures of alloy, melt-spun from 1723 and 1773 K, are composed of the Fe-rich amorphous matrix and Cu-rich spherical crystalline precipitates. For the higher melt-ejection temperature, no coarse precipitates could be observed. Amorphous nature of the Fe-rich matrix was confirmed by presence of a broad diffraction maximum on the X-ray diffraction patterns, a halo ring on the electron diffraction pattern as well as presence of exothermic effects, related to the crystallization of the Fe-rich amorphous matrix, in the differential scanning calorimetry. Beside presence of copper, revealing positive heat of mixing with iron, relatively large supercooled liquid region, was noticed.

Keywords: metallic glasses, amorphous-crystalline composites, melt-spinning

Praca przedstawia badania kompozytu amorficzno-krystalicznego otrzymanego w stopie $Fe_{66}Cu_6B_{19}Si_5Nb_4$. Badania obejmowały rentgenowską analizę fazową (XRD), skaningową kalorymetrię różnicową (DSC), mikroskopię świetlną (LM), skaningową mikroskopię elektronową (SEM) i transmisyjną mikroskopię elektronową (TEM). Odpowiedni dobór składu chemicznego umożliwił uzyskanie kompozytu amorficzno-krystalicznego dzięki wykorzystaniu zjawiska podziału w stanie ciekłym w efekcie dodatniego ciepła tworzenia roztworu pomiędzy żelazem i miedzią. Mikrostruktury badanego stopu, po odlaniu z temperatury 1723 i 1773 K, składają się z amorficznej osnowy bogatej w żelazo i krystalicznych kulistych wydzieleń bogatych w miedź. Dla wyższej temperatury odlewania nie obserwowano dużych wydzieleń. Obecność fazy amorficznej została potwierdzona poprzez obecność halo na dyfrakcji elektronowej oraz efekt cieplny egzotermiczny w badaniach skaningowej kalorymetrii różnicowej, związany z krystalizacją osnowy bogatej w żelazo. Pomimo dodatku miedzi, wykazującej dodatnie ciepło tworzenia roztworu z żelazem, wyznaczony zakres cieczy przechłodzonej jest względnie duży.

1. Introduction

Since the first reports of metallic glasses [1], there has been a great interest in their application as an engineering material. The main obstacle is brittleness of metallic glasses caused by intense localization of the plastic deformation into shear bands [2]. In order to improve their ductility, bulk metallic glass matrix composites has been developed [3,4]. The presence of a ductile crystalline phase encourages the formation of multiple shear bands and thus improves ductility. Such composites can be obtained either by ex-situ introduction of the reinforcing particles prior to casting [3], or by in-situ formation of the crystalline phases [4]. A spherical shape of precipitates is most desired from a point of view of ductility. It can not be achieved during in-situ heterogeneous nucleation from a liquid state.

The use of liquid phase separation phenomenon allows obtaining the amorphous-crystalline composites with a spherical shape of a crystalline phase [5,6]. This phenomenon occurs in alloys containing at least two elements with a high positive heat of mixing and consequently stable or metastable liquid miscibility gaps.

If a homogeneous melt, with a composition within the miscibility gap, is cooled below the critical temperature, a thermodynamic driving force for decomposition in a liquid state appears. Because of lack of elastic strain energy and relatively low surface energy between two melts, the precipitates tend to adopt a spherical shape. The continuous cooling decreases mutual solubility and induces precipitation process which is continued until the glass transition or the crystallization temperature is reached. If the glass forming ability of both melts are high enough, two-phase metallic glasses can be obtained [7-10]. However thermodynamic condition necessary for decomposition, decreases overall glass forming ability of an alloy, limiting maximum thickness of the material. If glass forming abilities of one of the melts will be not sufficient, the amorphous-crystalline composite can be obtained in-situ during cooling process [5,6,11].

In this paper the microstructures of the melt-spun $Fe_{66}Cu_6B_{19}Si_5Nb_4$ alloy are presented. This alloy is a modifi-

* AGH UNIVERSITY OF SCIENCE AND TECHNOLOGY, FACULTY OF METALS ENGINEERING AND INDUSTRIAL COMPUTER SCIENCE, AL. A. MICKIEWICZA 30, 30-059 KRAKOW, POLAND

** WARSAW UNIVERSITY OF TECHNOLOGY, FACULTY OF MATERIALS SCIENCE AND ENGINEERING, WOŁOSKA STREET 141, 02-507 WARSAW, POLAND

cation of the $Fe_{72}B_{19}Si_5Nb_4$ alloy, known as a relatively good glass former [12]. Partial substitution of iron with copper was expected to induce liquid phase separation due to a positive heat of mixing (Table 1). Since heats of mixing of other alloying elements are more negative to iron than copper, the Cu-rich melt was predicted to crystallize as a simple solid solution.

TABLE 1

The values of heat of mixing (kJ/mol) in liquid binary systems [13]

	Fe	Cu	Si	B	Nb
Fe	0	+13	-35	-26	-16
Cu		0	-19	0	+3
Si			0	-14	-56
B				0	-54
Nb					0

2. Experimental procedure

The alloy with a nominal composition of $Fe_{66}Cu_6B_{19}Si_5Nb_4$ (at. %) was prepared by arc melting of a mixture of high purity elements (99.9 % or higher) under titanium gettered argon atmosphere. Rapidly solidified alloys were prepared by the melt spinning technique (Edmund Bühler melt spinner HV) at a linear wheel speed of 40 m/s and a protective gas (argon) over-pressure of 50 kPa. Two melt-ejection temperatures, 1723 K (1450°C) and 1773 K (1500°C), were applied. This parameter was controlled using built-in infrared quotient pyrometer to measure the temperature of the melt in the process. Microstructure observations of the melt-spun ribbons were carried out on the cross sections of ribbons polished and etched with a solution consisting of 5g $FeCl_3$, 15g HCl and 200 ml distilled water. Light microscopy (LM) observations enabled to affirm if any inhomogenity, related to the miscibility gap, occurred. Detailed microstructure studies of the ribbons were carried out by means of scanning electron microscopy (SEM, Hitachi S-3500N) and transmission electron microscopy (TEM, JEOL JEM-200 CX). X-ray diffraction (XRD) studies were carried out using Siemens D500 diffractometer applying Cu-Kα monochromatic radiation (λCuKα =1.54 Å). Differential scanning calorimetry (DSC) measurements (PerkinElmer Pyris Diamond DSC) enabled thermal effects registration. The ribbons were heated within the temperature range from 323 to 1023 K applying heating rates of 20, 40 and 80 K/min. Glass transition (T_g), onset crystallization (T_x) and peak (T_p) temperatures as well as enthalpy of crystallization (ΔH) were determined from the DSC studies. The Tg temperatures were established from the inflexion point on the DSC curve. The activation energy (Q) was estimated from Kissinger plot. It was assumed that the error of estimation is equal to half-width of the confidence interval at significance level of 0.05.

3. Results and discussion

The microstructures of the examined alloy melt-spun from 1723 K and 1773 K, observed on the cross section of etched ribbons, are presented in Figures 1 and 2, respectively. No elongated lamellar region, typical for cooling from the liquid miscibility gap regions [11], were observed. However for the lower melt-ejection temperature spherical precipitates of few microns in diameter could be observed (Fig. 1). It indicates that these were formed in the upper range of the miscibility gap. Increase of the melt-ejection temperature up to 1773 K enabled to avoid presence of large precipitates (Fig. 2).
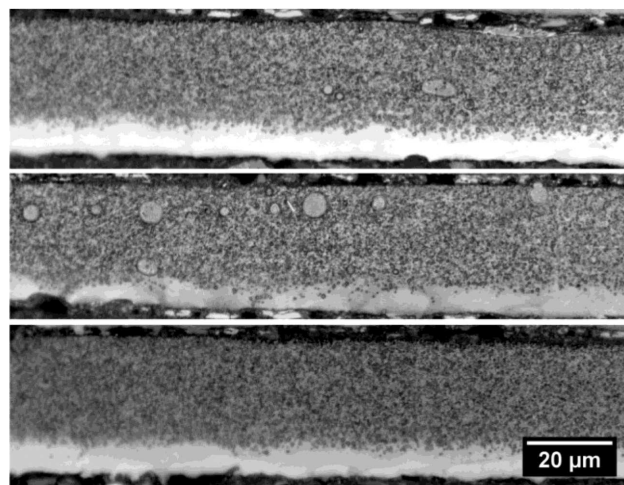

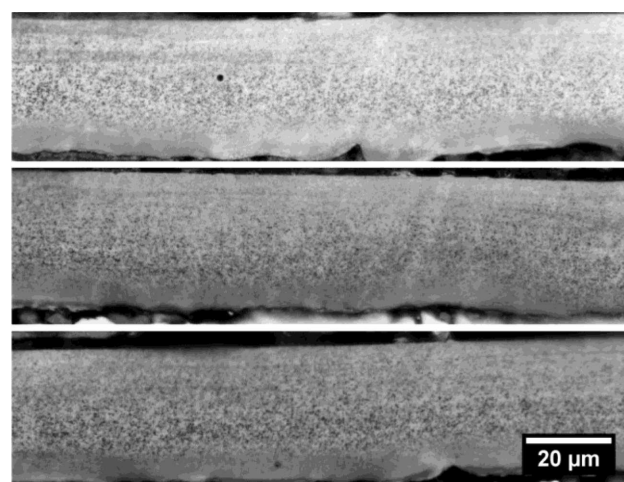Fig. 1. LM microstructures of the $Fe_{66}Cu_6B_{19}Si_5Nb_4$ alloy melt-spun from 1723 K (cross sections of the ribbons)

Fig. 2. LM microstructures of the $Fe_{66}Cu_6B_{19}Si_5Nb_4$ alloy melt-spun from 1773 K (cross sections of the ribbons)

SEM image of the ribbon melt-spun from 1723 K with corresponding EDS spectra of the matrix and large spherical precipitate are presented in Figure 3. The studies pointed out that the matrix is composed of the Fe-rich phase (Fig. 3b), whereas the spherical precipitates constitute the previously existing Cu-rich melt (Fig. 3c). Moreover very fine precipitates, with size below 1 um, were observed. However the EDS analysis of these precipitates could not be precisely estimated.
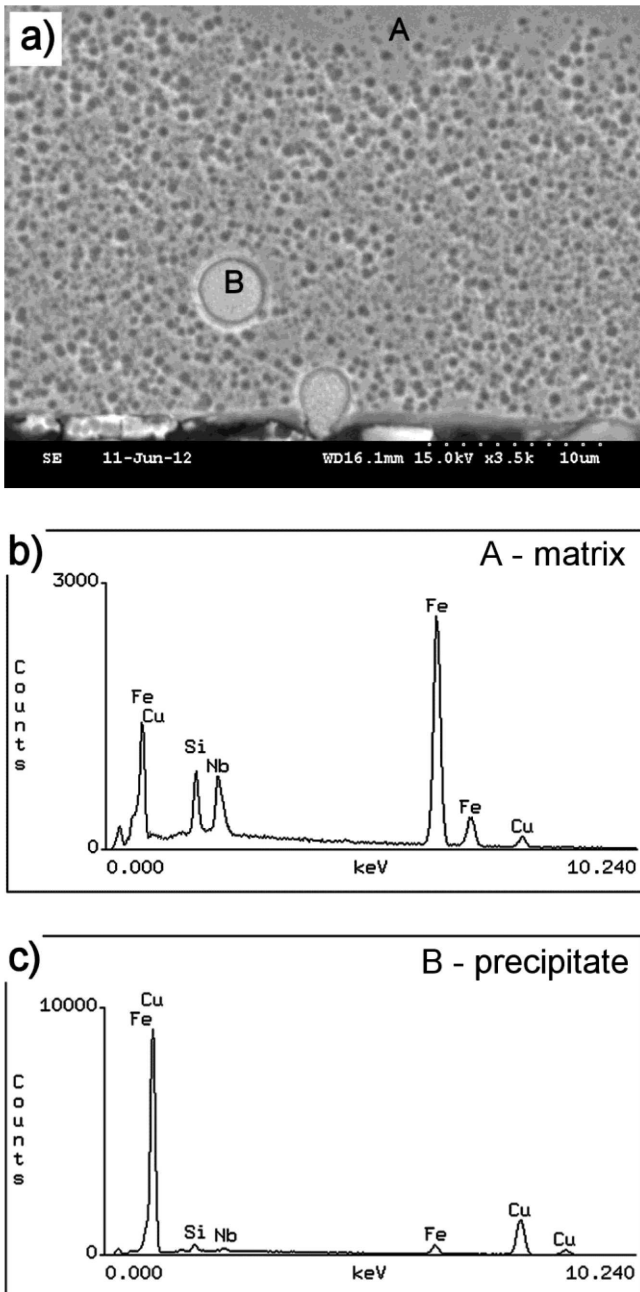
Fig. 3. a) SEM image of the examined $Fe_{66}Cu_6B_{19}Si_5Nb_4$ alloy melt-spun from 1723 K observed on the cross section with corresponding EDS spectra from b) matrix and c) spherical precipitate

Fig. 4. a,b) TEM bright field images of the examined $Fe_{66}Cu_6B_{19}Si_5Nb_4$ alloy melt-spun from 1723 K with SAED pattern from matrix (inset)

Fig. 5. XRD patterns of the $Fe_{66}Cu_6B_{19}Si_5Nb_4$ alloy melt-spun from 1723 and 1773 K

TEM bright field images, supported by selected area electron diffraction (SAED) pattern, of the ribbon melt-spun from 1723 K are shown in Figure 4. A halo ring observed on the SAED pattern from the matrix (Fig. 4a) indicates glassy nature of the Fe-rich matrix. The matrix is covered with very fine spherical precipitates with size below 100 nm. Therefore some crystalline spots could be observed on the SAED pattern.

The XRD patterns of the examined alloy melt-spun from 1723 and 1773 K are shown in Figure 5. In both ribbons only one crystalline phase, with a highest intensity maximum at $2\theta = 43.3°$ corresponding to the presence of the copper, was identified. However, it is expected that due to the formation in the liquid state, this phase is the Cu-rich solid solution instead of pure copper. A broad intensity maximum of peaks confirms presence of the amorphous phase.
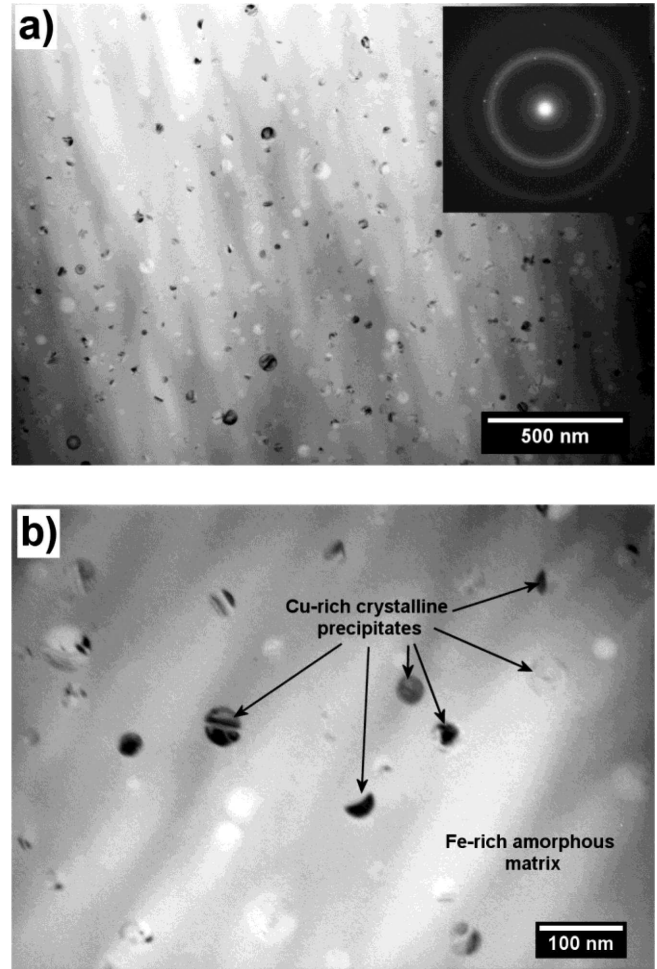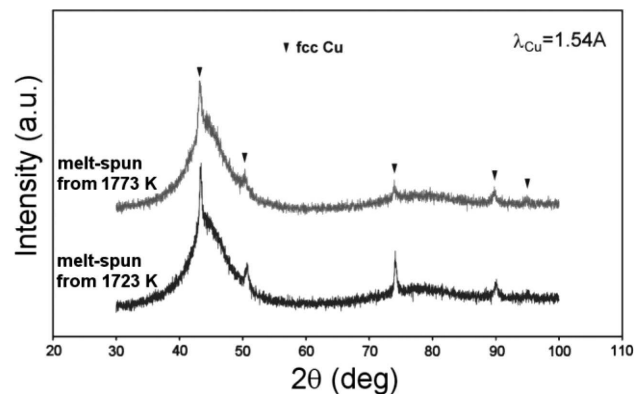
The DSC curves of the examined ribbons, recorded at a heating rate of 40 K/min, are presented in Figure 6. In both alloys exothermic peaks, related to the crystallization of the amorphous matrix, were observed. Detailed results of the DSC investigations are summarized in Table 2. The measured enthalpies of crystallization are relatively low, in comparison to the single-phase Fe-based metallic glasses, due to a presence of the Cu-rich crystalline phase. In case of the alloy melt-spun from 1723 K, only one exothermic peak was observed. In-

TABLE 2

Results of DSC measurements of the examined alloy melt-spun from 1723 and 1773 K

Melt ejection temperature (K)	Heating rate β (K/min)	T_g (K)	T_x (K)	T_{p1} (K)	T_{p2} (K)	ΔT_x (K)	ΔH_1 (J/g)	Q (kJ/mol)
1723	20	832	901	919	-	69	-85	364±67
	40	855	910	929	-	55	-95	
	80	885	925	945	-	40	-93	
1773	20	836	879	915	944	43	-16	-
	40	854	899	927	961	45	-39	
	80	877	920	941	1004	45	-43	

crease of the melt-ejection temperature to 1773 K changed crystallization behavior. It proves that the lower temperature was in the upper range of the liquid miscibility gap. Increase of the melt-ejection temperature by 50 K enabled to achieve a homogeneous melt region, which resulted in change of the chemical composition of the liquid alloy, consequently. The activation energy of crystallization of the amorphous phase in case of the ribbon melt-spun from 1723 K is as high as 364±67 kJ/mol. Relatively large supercooled liquid region before crystallization, ΔT_x, which is a temperature interval between glass transition temperature (T_g) and crystallization temperature (T_x), was noticed.

Fig. 6. DSC curves of the examined alloy melt-spun from 1723 and 1773K recorded at a heating rate of 40 K/min

4. Conclusions

- Rapid cooling of the examined $Fe_{66}Cu_6B_{19}Si_5Nb_4$ alloy, melt-spun from 1723 and 1773 K, enabled formation of the amorphous-crystalline composite, consisting the Fe-rich amorphous matrix and the Cu-rich crystalline precipitates.
- Increase of the melt-ejection temperature changed crystallization behavior of the amorphous phase and allowed to avoid presence of coarse precipitates.
- Cooling through the miscibility gap enabled to obtain spherical shape of crystalline precipitates.

- Size of the highest precipitates, observed by means of light microscopy, was in the range of 10 μm, whereas the smallest ones, observed in thin foil, were far below 100 nm.
- Beside presence of copper, which is expected to decrease overall glass forming ability of the alloy, relatively large supercooled liquid region, ΔT_x, was noticed.

REFERENCES

[1] W. Klement, R.H. Willens, P. Duwez, Non-crystalline structure in solidified gold-silicon alloys, Nature **187**, 869-870 (1960).

[2] R.D. Conner, R.B. Dandliker, W.L. Johnson, Mechanical properties of tungsten and steel fiber reinforced $Zr_{41.25}Ti_{13.75}Cu_{12.5}Ni_{10}Be_{22.5}$ metallic glass matrix composites, Acta Mater. **46**, 6089-6102 (1998).

[3] F. Szuecs, C.P. Kim, W.L. Johnson, Mechanical properties of $Zr_{56.2}Ti_{13.8}Nb_{5.0}Cu_{6.9}Ni_{5.6}Be_{12.5}$ ductile phase reinforced bulk metallic glass composite, Acta Mater. **49**, 1507-1513 (2001).

[4] H. Tan, Y. Zhang, Y. Li, Synthesis of La-based in-situ bulk metallic glass matrix composite, Intermetallics **10**, 1203-1205 (2002).

[5] T. Kozieł, Z. Kędzierski, A. Zielińska-Lipiec, K. Ziewiec, The microstructure of liquid immiscible Fe-Cu-based in situ formed amorphous/crystalline composite, Sc1r. Mater. **54**, 1991-1995 (2006).

[6] K. Ziewiec, P. Malczewski, R. Gajerski, A. Ziewiec, The microstructure development in arc-melt and melt-spun $Fe_{50}Ni_{10}Cu_{20}P_{10}Si_5B_5$ immiscible alloy, J. Non-Cryst. Solids **357**, 73-77 (2011).

[7] A.A. Kündig, M. Ohnuma, D.H. Ping, T. Ohkubo, K. Hono, In situ formed two-phase metallic glass with fractal microstructure, Acta Mater. **52**, 2441-2448 (2004).

[8] B.J. Park, H.J. Chang, D.H. Kim, W.T. Kim, In situ formation of two amorphous phases by liquid phase separation in Y-Ti-Al-Co alloy, Appl. Phys. Lett. **85**, 6353-6355 (2004).

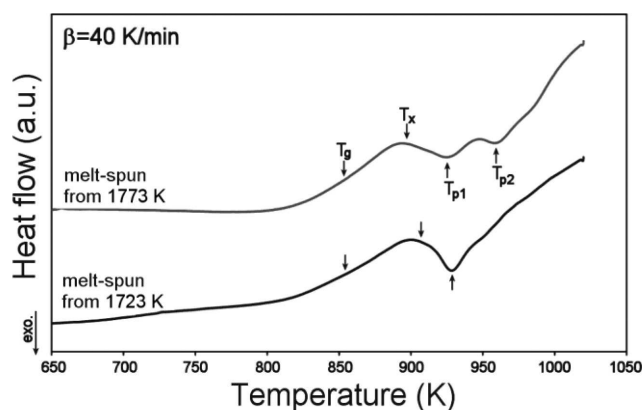[9] N. Mattern, U. Kühn, A. Gebert, T. Gemming, M. Zinkevich, H. Wendrock, L. Schultz, Microstruc-

ture and thermal behavior of two-phase amorphous Ni-Nb-Y alloy, Scr. Mater. **53**, 271-274 (2005).

[10] E.S. P a r k, J.S. K y e o n g, D.H. K i m, Phase separation and improved plasticity by modulated heterogeneity in Cu-(Zr,Hf)-(Gd,Y)-Al metallic glasses, Scr. Mater. **57**, 49-52 (2007).

[11] T. K o z i e ł, A. Z i e l i ń s k a - L i p i e c, J. L a t u c h, S. K ą c, Microstructure and properties of the in situ formed amorphous-crystalline composites in the Fe-Cu-based immiscible alloys, J. Alloys Compd. **509**, 4891-4895 (2011).

[12] Y.R. Z h a n g, R.V. R a m a n u j a n, The effect of niobium alloying additions on the crystallization of a Fe-Si-B-Nb alloy, J. of Alloys Compd. **403**, 197-205 (2005).

[13] A. T a k e u c h i, A. I n o u e, Classification of bulk metallic glasses by atomic size difference, heat of mixing and period of constituent elements and its application to characterization of the main alloying element, Mater. Trans. **46**, 2817-2829 (2005).